

PAPER • OPEN ACCESS

Experimental Study of Gaseous Flames Issuing from a Conically Stabilized Swirl Burner Using Prevaporized Partially Premixed Biodiesel and Diethyl Ether

To cite this article: H S Mohamed *et al* 2025 *J. Phys.: Conf. Ser.* **3058** 012016

View the [article online](#) for updates and enhancements.

You may also like

- [Establishing ideal CI engine input parameters for optimal engine output characteristics utilizing experimental and optimization techniques for series-hybrid powertrain](#)
Sinnappadass Muniyappan, Shishir Kumar Behera and Ravi Krishnaiah
- [A gravimetric approach to providing SI traceability for concentration measurement results of mercury vapor at ambient air levels](#)
Hugo Ent, Inge van Andel, Maurice Heemskerk *et al.*
- [Investigation on Performance and Emission of Pongamia Biodiesel Using Diethyl Ether and Zinc Oxide as Additive in Diesel Engine](#)
K Rajesh, P K Devan, B Lokesh *et al.*

 The Electrochemical Society
Advancing solid state & electrochemical science & technology

UNITED THROUGH SCIENCE & TECHNOLOGY

248th ECS Meeting Chicago, IL October 12-16, 2025 *Hilton Chicago*



Science + Technology + YOU!

Register by September 22 to **save \$\$\$**

[REGISTER NOW](#)

Experimental Study of Gaseous Flames Issuing from a Conically Stabilized Swirl Burner Using Prevaporized Partially Premixed Biodiesel and Diethyl Ether

H S Mohamed¹, H A MONEIB², A M A Attia³ and R M El-Zoheiry³

¹ Egyptian Atomic Energy Authority, Hot Labs Center, Inshas, Cairo, Egypt

² Mechanical Power Engineering Department, Faculty of Engineering, Helwan University, Mattaria, Egypt

³ Mechanical Engineering Department, Faculty of Engineering, Benha University, Benha, Egypt

E mail: hassan1966sadek1931@gmail.com

Abstract. This study investigates the effects of blends of diethyl ether, biodiesel, and Jet A-1 fuel on exhaust emissions and flame characteristics in a conical swirl burner. The tested fuels included pure Jet A-1 fuel (B0) and blends of diethyl ether and biodiesel (B5, B10, B5D40, and B10D40), where biodiesel was produced from used waste cooking oil via an ultrasound-assisted transesterification process. The fuel-air mixture was pre-vaporized at 300°C and burned in a cylindrical combustion chamber (diameter-to-length ratio of 3.75:12.5) using a screw burner (swirl number: 0.55) with a lean equivalence ratio (ϕ) of 0.80. Key parameters analyzed were exit temperature, CO, O₂ concentration, NO_x emissions, blend ratio (BR), fuel flow rate, and local equivalence ratio (ϕ_{local}). As ϕ_{local} approached stoichiometry ($\phi_{local} = 1.0$), chamber temperatures increased, while NO_x and CO concentrations decreased. Conversely, when ϕ_{local} neared the overall equivalence ratio (0.80), exit temperatures and NO_x levels dropped but CO levels rose. Increasing the blend ratio, which raises the waste cooking oil methyl ester (WCOME) content, led to lower temperatures and higher CO emissions. All tests achieved stable flames, with the highest temperature of 1570 K using the B10 blend. Adding 40% diethyl ether to the blends notably reduced emissions and improved flame temperature, making this blend ratio ideal for better emission control and flame performance.

Keywords: Gaseous Flames, Conically Stabilized Swirl Burner, Prevaporized Partially Premixed, Biodiesel, Diethyl Ether.

1. Introduction

Fossil fuels are approaching depletion in the near future due to rising consumption rates across all areas of life [1]. This trend contributes to the worsening phenomenon of global warming and climate change, which is exacerbated by increasing environmental pollution and the spread of dangerous diseases that threaten human health [2]. The use of fossil fuels is a significant factor in these issues [3]. In contrast, biodiesel fuel offers several advantages over conventional diesel fuels [4]. It is biodegradable, has a higher flash point and cetane content, is non-toxic, and produces lower emissions of carbon monoxide, hydrocarbons, and unburned particulate matter. Additionally, biodiesel contains lower levels of sulfur and volatile organic compounds [5].

The raw materials for diesel fuel production are classified into three generations, as shown in Table 1 [3,4-17]. The first generation relies on raw materials such as castor oil, rapeseed, soybean,



edible oils, and palm oil [7]. This generation poses a threat to global food security due to its dependence on edible oils for biodiesel production [9]. Consequently, researchers have sought to produce biodiesel from non-edible oil crops, leading to the development of second-generation feedstocks like jatropha and jojoba [10]. However, a significant challenge for this generation is the limited cultivation of these crops [11]. The third generation of raw materials aims to address the challenges faced by previous generations, focusing on the availability of these resources, economic feasibility, and their impact on the food chain [12].

Research and laboratory findings indicate that using pure biodiesel and blending it with fossil fuels in various ratios has resulted in a notable reduction in harmful and toxic emissions. This includes decreases in carbon monoxide (CO), unburned hydrocarbons (UHC), and smoke levels, alongside an increase in emissions of carbon dioxide (CO₂) and nitrogen oxides (NO_x) [13]. Additionally, employing advanced combustion improvement techniques can further reduce pollutant emissions. One promising method is lean combustion (LPP), which involves using pre-mixed, pre-vaporized combustion techniques instead of diffusion combustion to simplify the combustion process [14].

Table 1. Raw materials used in the production of biodiesel [3].

Feedstocks for biodiesel production :		
Edible oil (1 st generation)	Non – edible oil (2 nd generation)	Other sources (3 rd generation)
Rapeseed oil [4, 12]	Jatrophacurcus [7,14]	Waste cooking oil [9,16]
Palm oil [5 ,13]	Jojoba [8,15]	Chicken fat oil [10,15]
Castor oil [6 ,13]		Fish oil [11, 17]
Soybean oil [7 ,14]		Micro algae [11, 17]

Table 2 presents the findings of previous research on the factors influencing emission rates from biodiesel combustion [15]. The most significant factor is high viscosity, which increases carbon dioxide emissions. Conversely, factors like oxygen can elevate temperature and reduce these emissions [16]. Among combustion technologies, pre-mixed and vaporized combustion (LPP) is optimal for minimizing toxic emissions while ensuring high combustion quality [17]. The combustion process characteristics and its environmental impact serve as key criteria for comparing and selecting fuel types for aircraft gas turbines [18].

Table 2. Results of previous research on emissions from biodiesel combustion.

Biodiesel type	T	CO	NO _x	Ref.
Jojoba oil biodiesel-Jet-A1 blends	Decrease	Increase	Decrease	El-Zoheiry [18]
Waste cooking oil methyl ester and Jet A-1	Decrease	Increase	Decrease	Belal [19]
(WCOME) with Jet A-1 (symbolized as B5, B10, B15, and B20)	Increase: at (B20)	Decrease: at (B20)	Decrease : at (B20)	Attia [20]
Canola methyl ester	Decrease		Decrease	Jr [21]
Sunflower oil biodiesel	Increase	Decrease	-----	San José [22]
Soybean and Sunflower oils	Decrease	Increase	Decrease	Ghorbani [23]
Pome	Increase	Decrease	Increase	Ng [24]
Soybean and animal fat oils	Increase	Decrease	Decrease	Panchasara [25]

There is a significant lack of research and studies on the combustion characteristics of three-phase fuel mixtures using a stabilized conical swirl burner. The objective of this study is to produce biodiesel from waste cooking oil, enhance stable flame combustion, and reduce harmful gaseous emissions—especially nitrogen oxides and carbon monoxide—during the combustion of fuel blends containing biodiesel, jet (aviation) fuel, and diethyl ether, using a stabilized conical swirl burner.

1.1. NO_x Formation and Destruction in Flame

The thermodynamics and kinetics of nitrogen oxides (NO and NO₂, collectively referred to as NO_x) formation and destruction through their conversion to molecular nitrogen (N₂) are discussed in excellent reviews [19].

1. The three principal sources of NO_x in the combustion of fossil fuels are [21]:
2. Thermal or Zeldovich NO: The fixation of atmospheric (molecular) nitrogen by atomic oxygen at high temperatures in oxidizing atmospheres.
3. Prompt NO: The fixation of atmospheric (molecular) nitrogen by hydrocarbon fragments in reducing atmospheres.
4. Fuel NO: The oxidation of nitrogen compounds that are organically bound in the fuel.

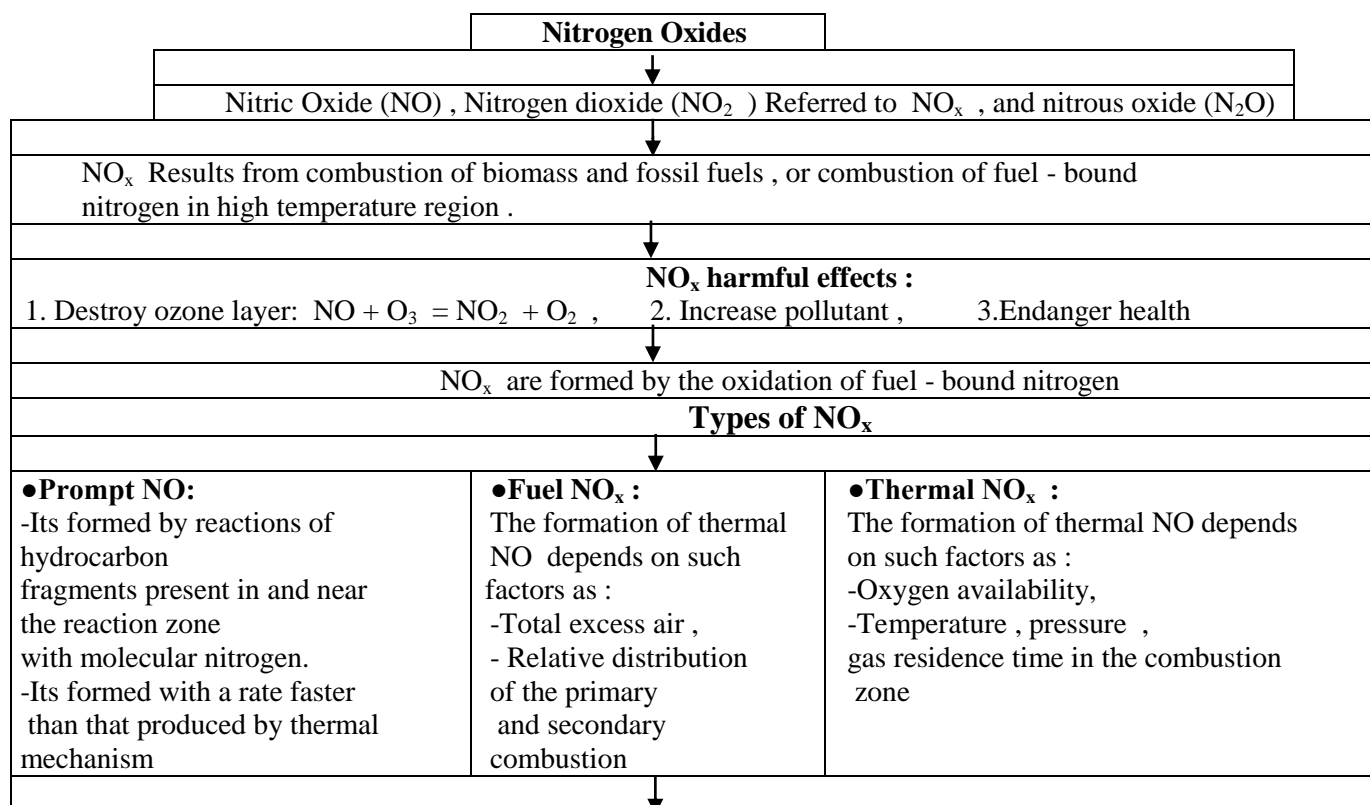
The various mechanisms for NO_x formation are illustrated in the flow chart in figure 1 [22].

Thermal NO

This reaction mechanism was first identified by Zelovich [23] as an atom shuttle reaction:

1. $\text{N}_2 + \text{O} \rightarrow \text{NO} + \text{N}$ (1)
2. $\text{N} + \text{O}_2 \rightarrow \text{NO} + \text{O}$ (2)
3. $\text{N} + \text{OH} \rightarrow \text{NO} + \text{H}$ (3)

Due to the high activation energy of reaction (1), NO production through this mechanism occurs at a slower rate than the oxidation of the fuel constituents and is highly temperature sensitive. Consequently, the Zelovich mechanism predominates in fuel-lean, high-temperature systems [24].



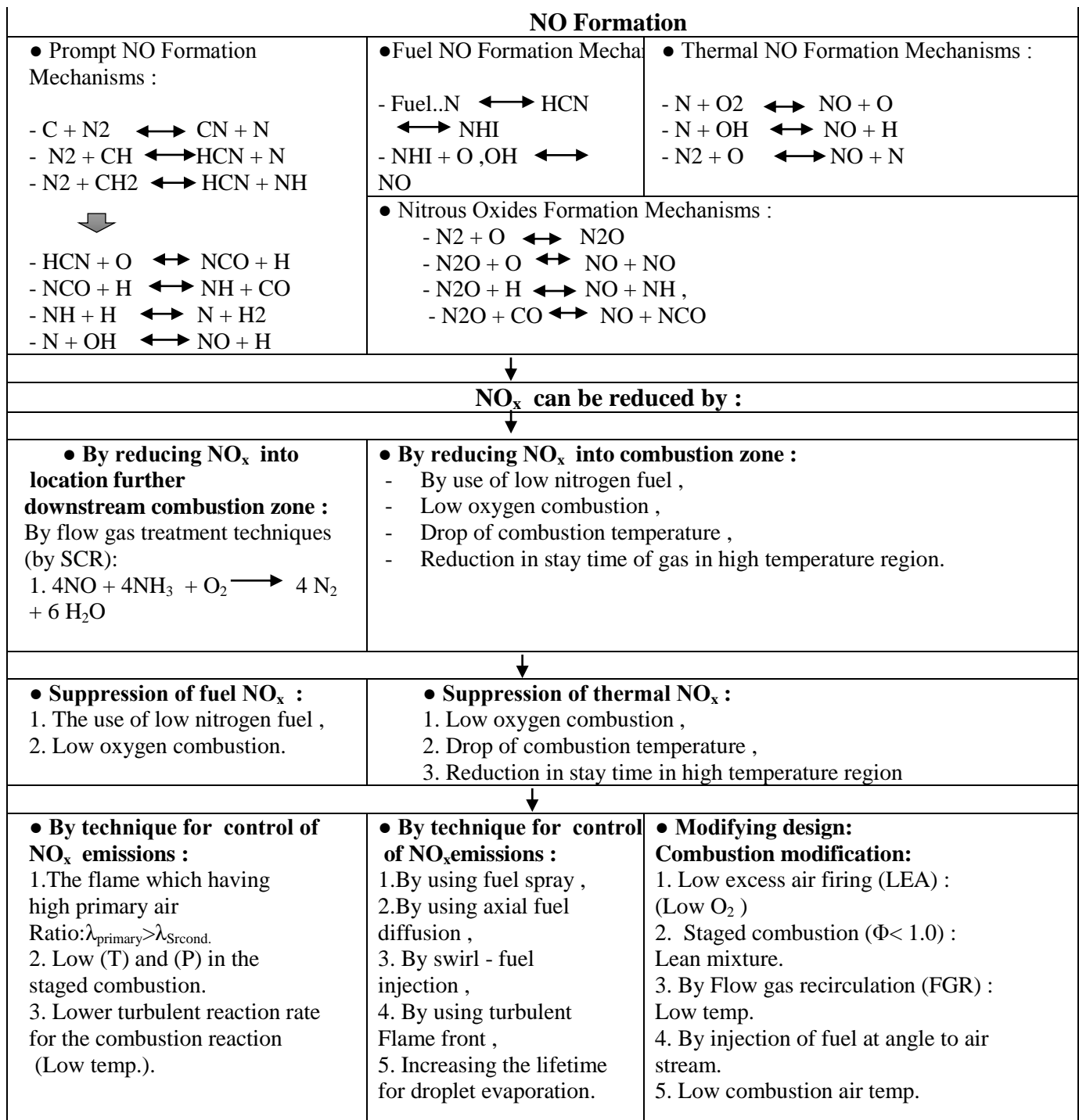


Figure 1. Flow chart of (NO_x) formation schemes and reduction techniques [26-30].

Flame structure shown in figure 1.2, the flame may be divided into the following regions or zones ;

- Preheating zones ,
- Primary reaction zone ,
- Internal zone ,

• Secondary reaction zone .

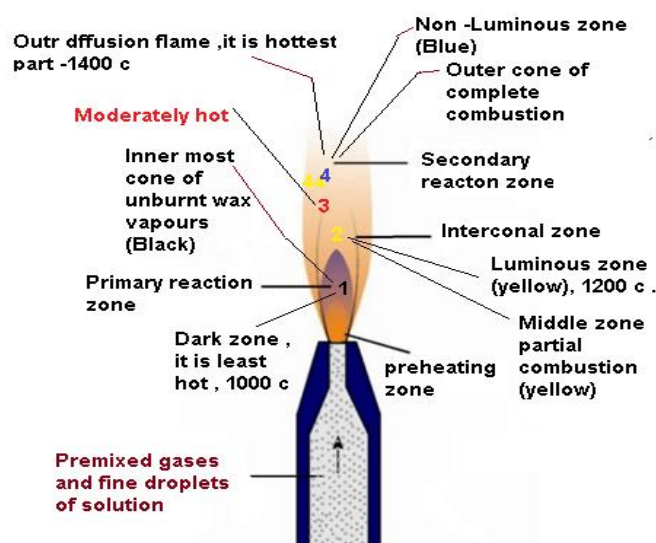


Figure 2. Flame characterization by different zones of flame structures.

1.2. Biodiesel Production Process

Preparation Steps for Biodiesel from Waste Cooking Oil (1 Liter) [31]. Waste Cooking Oil Sample Preparation:

1. **Collection and Filtration:** Waste cooking oil was sourced from households and restaurants, primarily consisting of palm and sunflower oil, and filtered to remove food particles.
2. **Heating the Oil:** The filtered oil was heated to 60°C using a magnetic stirrer for 15 minutes to eliminate impurities (Figure 2).
3. **Catalyst Solution Preparation:** A catalyst solution was made by dissolving 10 grams of potassium hydroxide (KOH) or 5 grams of sodium hydroxide (NaOH) in 330 ml of methanol, then added to the heated oil (Figure 2).
4. **Blending and Separation:** The oil-catalyst mixture was blended in an ultrasonic blender for 25 minutes, leading to the formation of a dark brown layer and subsequent separation of glycerol in a separating funnel (Figures 2 and 3).
5. **Washing and Drying:** The mixture was washed with a solution of water and vinegar, drained until clear, and finally heated above 100°C to evaporate remaining water, resulting in clear biodiesel (Figures 4 and 5).



Figure 2. Magnetic stirring with lab mixture: Ultrasonic setup (Transesterification).



Figure 3. Settling and Separation process (Biodiesel + Glycerol).



Figure 4. Water washing process (Washed biodiesel).

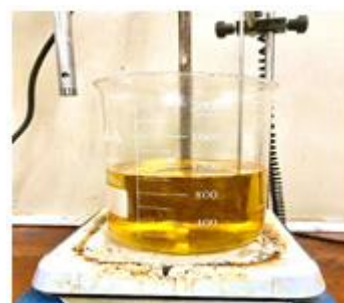
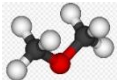
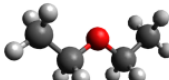
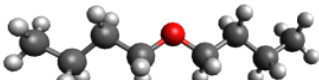


Figure 5. Waste cooking oil biodiesel

1.3. Ether fuels

Ether fuels are emerging as viable alternatives to traditional fossil fuels, primarily due to their potential for reduced emissions and compatibility with existing engine technologies. These fuels, derived from various ether compounds, exhibit favorable combustion properties and can be synthesized from renewable resources, making them an attractive option for sustainable energy solutions. The types of Ether Fuels are Diethyl ether (DEE, $C_4H_{10}O$), Dimethyl ether (DME, C_2H_6O) and Di-n-butyl Ether (DBE, $C_8H_{18}O$), see Table 3. Diethyl ether (DEE) and dimethyl ether (DME) are the most widely used ether fuels as alternative feedstock's and additives for diesel fuel, thanks to their shorter carbon chains and potential for improved ignition [32]. DEE, in particular, possesses properties similar to DME but remains liquid at room temperature, allowing its drawbacks to be mitigated by blending it with biodiesel [33]. Additionally, DEE is cheaper to produce than DME. A promising biofuel, diethyl ether ($[C_2H_5]_2O$), can be synthesized by dehydrating ethanol using solid acid catalysts [34].

Table 3. Analysis of the Properties of Dimethyl Ether (DME), Diethyl Ether (DEE), and (DBE) [35].

Property	DME	DEE	DBE
Chemical Formula	$(CH_3)_2O$	$(C_2H_5)_2O$	$(CH_3(CH_2)_3)_2O$
Structure			
Specific gravity at 15°C	0.668	0.715	0.773
Viscosity at 40°C, cSt	0.224	0.23	0.23
Flash Point °C	-41	-40	25
Boiling point °C at 1 atm	-25	34.6	142
Cetane Number	□55-60	□120	□91
Lower calorific value, MJ/kg	28.43	36.84	42.8
Molecular weight, kg/kmol	46.07	74.12	130.2
Elemental analysis, % by			
Carbon	52.2	64.9	-
Hydrogen	13	13.5	-
Sulfur	Nil	Nil	-
Oxygen	34.8	21.6	12.3
Nitrogen	Nil	Nil	-
Stoichiometric air/fuel ratio	8.9	11.1	-

2. Experimental

2.1. Experimental Test Rig

To investigate the combustion characteristics of waste cooking oil (WCO) and jet fuel blends using the premixed prevaporized combustion technique, a suitable combustor test rig has been constructed and equipped with the necessary measuring instruments. Figure 6 shows a schematic drawing of the combustor test rig.

The current test facility consists of four main systems:

1. Air Delivery System
2. Air Heating System
3. Fuel Supply System
4. Combustor

The following subsections provide more details about these systems.

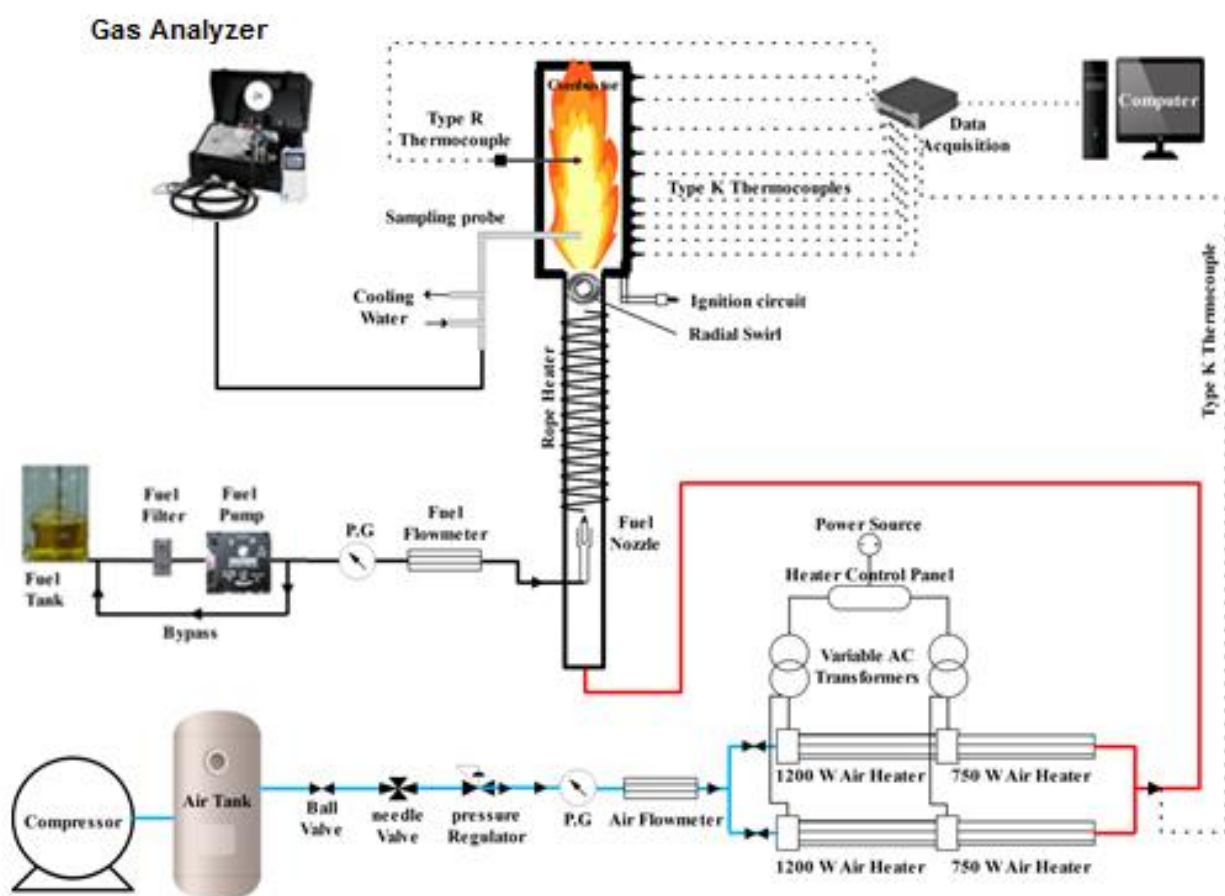


Figure 6. Test rig schematic drawings.

2.2. The Combustor

The combustor used in this study consists of two main components: (i) a confinement tube and (ii) a conical burner (see Figure 6). The confinement tube is designed to surround the swirl conical burner, creating a lean premixed prevaporized combustor. Its dimensions are aligned with those used in previous studies.

The ratio of the tube diameter (DT) to the conical burner diameter (DB) is set at 3.75, while the tube length to burner diameter ratio (LT/DB) is 12.5. Specifically, DT is 15 cm and LT is 50 cm.

Species concentrations were measured at designated points using an ECOM multi-gas analyzer. Flame temperatures were recorded at specific locations with a calibrated type B thermocouple (100

μm wire diameter, 0.6 mm bead diameter). Wall temperatures were monitored using ten calibrated K-type thermocouples positioned along the combustor wall.

3. Results and Discussion

This section presents the experimental results related to the combustion characteristics of the tested fuels using a lean premixed prevaporized combustion test facility. The results are analyzed and discussed in comparison to similar findings cited in the literature. A series of experiments were conducted to measure temperature and estimate thermal combustion efficiency across different fuel blending ratios (B0, B5, and B10). The experiments were performed under constant conditions, with an equivalence ratio of $\Phi_{\text{overall}}=0.80$ and a constant air flow rate of 0.474 kg/min, at an air preheating temperature of 573 K. Additionally, the temperature distribution along both the radial axis (r mm) and vertical axis (x mm) of the combustor was studied for different blending ratios while maintaining a constant equivalence ratio. Flame temperature was measured using a type B thermocouple (Pt/Pt-Rh 13%). The effect of the blending ratio (B0, B5, and B10) on the flame temperature distribution across various combustion zone locations was also investigated.

3.1. Distribution of Flame Temperature and Gaseous Emissions

Figures 7-9 demonstrate the differences in flame structure between fuel jet A-1 (B0) and biodiesel (B5 and B10). This variation is attributed to the lower flash point of fuel jet A-1 (39°C) compared to the flash point of waste cooking oil methyl ester (WCOME, 130°C). The contour figures indicate that flame temperature decreases uniformly from the burner's center to its outer radius. At the outer radius, flame temperatures drop consistently due to the angular momentum generated by the swirler. This causes the biodiesel (5% WCOME/B5 and 10% WCOME/B10) to burn as liquid droplets in a rich mixture ($\phi_{\text{local}} > 1.0$). In contrast, fuel jet A-1 (B0) and its mixes with biodiesel (95% jet/B5 and 90% jet/B10) burn as liquid vapor in a lean mixture ($\phi_{\text{local}} < 1.0$).

In all experiments, a higher proportion of biodiesel (WCOME) in the jet fuel (Jet A-1), as seen in blends B5 and B10, results in increased density and viscosity of the fuel mixture. This change delays the time for prevaporization and burning velocity, altering the properties and structure of the flame. The combustion of biofuels using swirl burner (SB) has been presented, and the corrected flame temperature distributions at selected vertical planes for the blended fuels are shown in Figures 7-9 and 10.a-d. It is important to note that the degree of mixture heterogeneity—and thus the potential for purely premixed or partially premixed combustion of blended fuels—primarily depends on the higher boiling point of the biodiesel.

The variations in temperature, NO_x , $\text{O}_2\%$, and CO with respect to ($x/X\%$) are illustrated in figures 10.a-d. Temperature decreases as ($x/X\%$) increase until reaching a minimum value, as shown in figure 11.a. The ($x/X\%$) values at which the minimum temperature occur vary depending on the fixed fuel flow rate or overall equivalence ratio (lean-0.80).

Additionally, the decrease in temperature at the burner outlet ($x/X\% = 98\%$) is attributed to an increase in ϕ_{local} approaching a lean mixture ($\phi_{\text{local}} = \phi_{\text{overall}} = 0.80$), leading to a dilution effect and increased total air concentration at the burner outlet. The peak temperature occurs at ($r/R\% = 0$ and $x/X\% = 0$) due to the swirled flow generating reversed and recirculating flow, producing spherical symmetric flames and flame cavities with liquid vapors (90% jetA-1/B10, 95% jetA-1/B5, and 100% jetA-1/B0) and liquid droplets (10% WCOME/B10 and 5% WCOME/B5). In these conditions, the oxidant, fuel droplets, and vapor react stoichiometrically, resulting in maximum flame temperature.

Such variation in figures (10-11: 10.b-10.d and 11.b-11.d) generally follows the same pattern across all figures. The temperature increases with an increase in ($x/X\%$) until it reaches a peak value; afterwards, the temperature drops. The values of ($x/X\%$) at which the peak temperature occurs vary with changes in local fuel flow rate or local equivalence ratio.

It is noteworthy that for a fixed fuel flow rate, the mixture in the local combustion zone becomes stoichiometric when the following relation is satisfied: $\phi_{\text{local}} = \phi_{\text{stoich}}$ when ($x/X\% = 10\text{--}40\%$). The increase in temperature with rising ($x/X\%$) is due to the local equivalence ratio (ϕ_{local})

approaching the stoichiometric value. Conversely, the decrease in temperature after this peak occurs due to an increase in local air concentration until the local equivalence ratio (ϕ_{local}) reaches an overall equivalence ratio of $\phi_{\text{local}} = 0.80$ at the burner outlet.

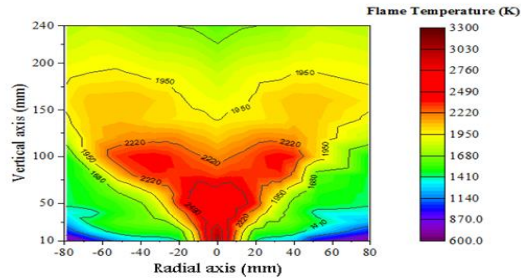


Figure 7. Contour of the distribution flame temperature (k) along the radial and vertical axis at $\phi = 0.80$ for B0 .

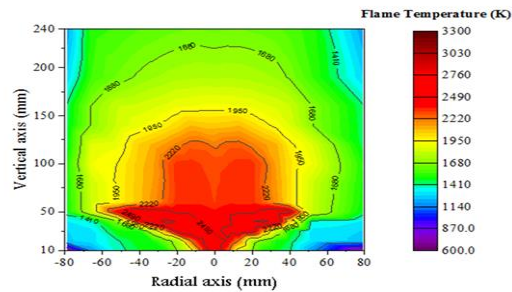


Figure 8. Contour of the distribution flame temperature (k) along the radial and vertical axis at $\phi = 0.80$ for B5 .

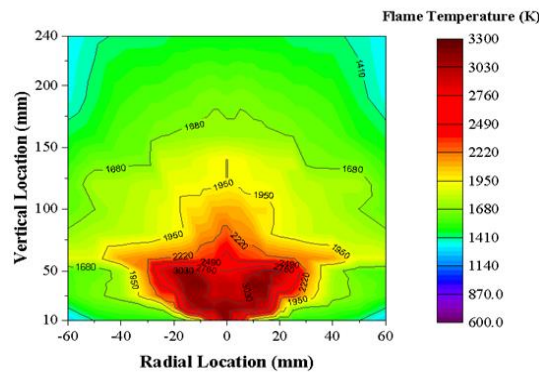
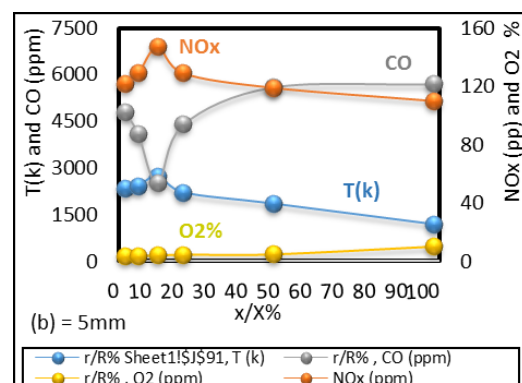
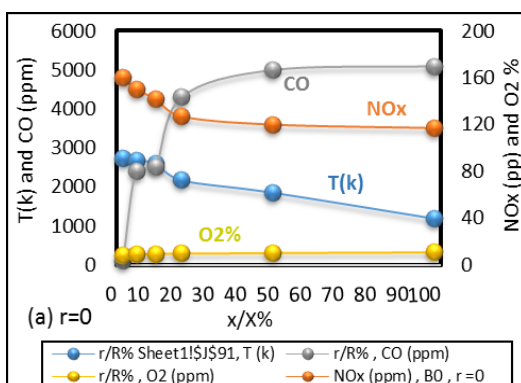


Figure 9. Contour of the distribution flame temperature (k) along the radial and vertical axis at $\phi = 0.80$ for B0 and B10 .



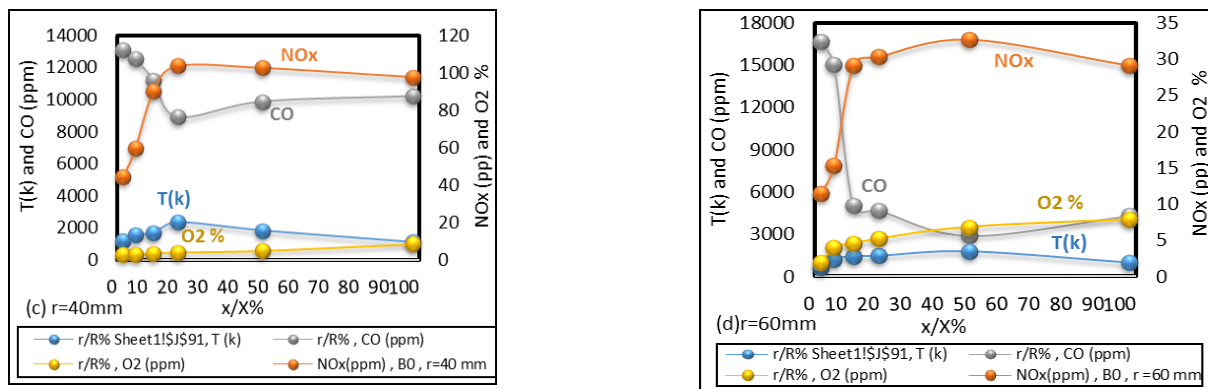


Figure 10. Relation between $T(K)$, NO_x (ppm), O_2 % and CO (ppm) at different x/X % and constants $r=0, 10, 40$ and 60 mm, equivalence ratio (ϕ)=0.75, B0, B5 and B10.

3.2. Combustion and Emission Characteristics of Adding Diethyl Ether to Bio-Cooking Oil Waste and Biodiesel

Figures 11. a-d, illustrate the temperature variation with respect to (x/X %) for the fuels B0, B5, B10, B0D40, B5D40, and B10D40. The temperature (K) decreases with increasing values of x/X %, as shown in Figure 11.a. This decrease can be attributed to the lean mixture at the combustor outlet, as depicted in Figures 11.a-d. Conversely, Figure 11.b-d indicate that the temperature initially increases with increases x/X % until a peak value is reached, after which the temperature declines. This trend occurs as temperature increases to a peak at $\phi_{local} = \phi_{stioch} = 1.0$, followed by a drop as $\phi_{local} = \phi_{overall} = 0.80$, indicating a lean mixture.

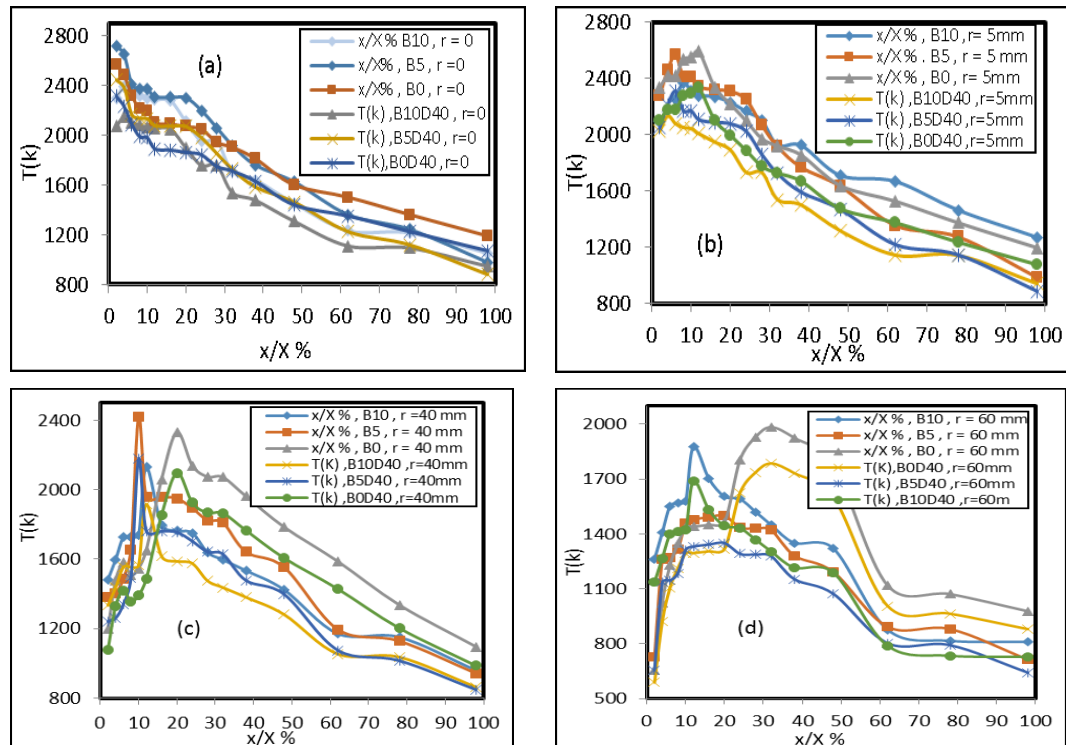


Figure 11. Axial distribution of flame temperature measurements for test fuels B0, B5, B10, B0D40, B5D40, and B10D40 throughout the combustor at an overall equivalence ratio of 0.80, and radial positions of 0, 5, 10, 15, 25, 30, 40, 50, and 60 mm.

Figures 12.a-d illustrate the variation of CO emissions (ppm) with respect to ($x/X\%$) for the fuel blends B0, B5, B10, B0D40, B5D40, and B10D40. As shown in figures 12.a, CO (ppm) increases with increasing $x/X\%$. This increase is attributed to a decrease in temperature until it reaches a lean value at ($\phi_{\text{local}} = \phi_{\text{overall}} = 0.80$) at the combustor outlet ($x/X\% = 98\%$). Figures 12.b and d reveal that CO (ppm) decreases with increasing ($x/X\%$) until it reaches a minimum value, after which it begins to rise again. This behavior corresponds to an increase in temperature until it peaks at ($\phi_{\text{local}} = \phi_{\text{stoich}} = 1.0$), followed by a decrease in temperature in the outlet direction of the burner. At this point, the conditions define a lean mixture: ($\phi_{\text{local}} = \phi_{\text{overall}} = 0.80 < 1.0$). The CO (ppm) emissions for B0D40, B5D40, and B10D40 are lower than those for B0, B5, and B10, respectively. This reduction is due to lower carbon contents, heating values, viscosity turbulence, and an increase in turbulence intensity, pre-vaporization, and burning velocity in the blends containing biodiesel (B0D40, B5D40, and B10D40). Specifically, B0D40 shows lower CO (ppm) compared to B5D40 and B10D40, linked to reduced viscosity turbulence, lower boiling point temperature, and enhanced pre-vaporization and burning velocity.

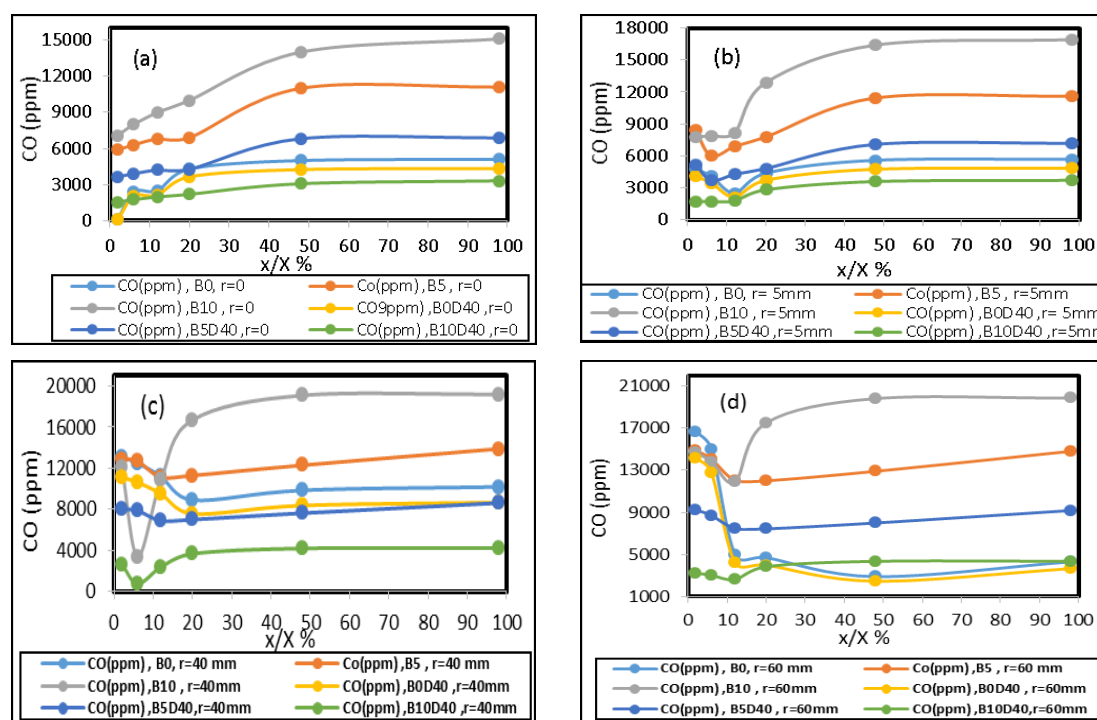


Figure 12. Axial distribution of CO concentration throughout the combustor at at $\phi_{\text{overall}} = 0.80$ and at radial distances of $r=0,5,10,15,25,30,40,50$, and 60 mm.

Figures 13.a-d illustrate the variation of NO_x (ppm) with respect to ($x/X\%$) for fuel blends B0, B5, B10, B0D40, B5D40, and B10D40. As shown in Figure 13.a, NO_x (ppm) decreases with increasing $x/X\%$, primarily due to a reduction in temperature until it reaches a lean value at ($\phi_{\text{local}} = \phi_{\text{overall}} = 0.80$) at the combustor outlet ($x/X\% = 98\%$). Figures 13.b and d indicate that NO_x (ppm) initially increases with increase $x/X\%$ until it reaches a maximum, after which it declines as temperature increases, peaking at ($\phi_{\text{local}} = \phi_{\text{stoich}} = 1.0$). Beyond this point, temperature decreases at ($\phi_{\text{local}} = \phi_{\text{overall}} = 0.80$), indicating a lean mixture. The NO_x (ppm) emissions for B0D40, B5D40, and B10D40 are lower than those of B0, B5, and B10, respectively. This reduction is attributed to factors such as lower temperature, heating value, turbulence intensity, viscosity, and reduced nitrogen and oxygen content, along with increased burning velocity in the biodiesel blends.

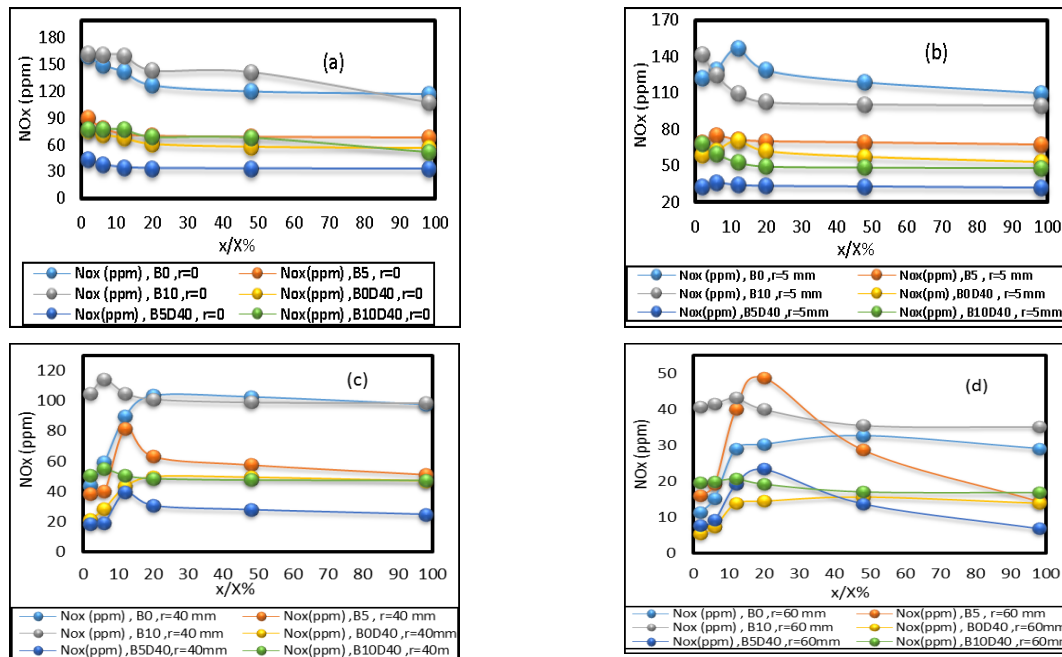


Figure 13. shows the axial distribution of NO_x concentration throughout the combustor at $\phi_{\text{overall}} = 0.80$ and radial distances of $r = 0, 5, 10, 15, 25, 30, 40, 50$, and 60 mm.

Specifically, NO_x emissions for B10D40, B5D40, and B0D40 are lower than those for B0, B5, and B10 due to decreased heating value, boiling point temperature, and viscosity, alongside increased prevaporized turbulence and oxygen content. Among these, B0D40 exhibits the lowest NO_x (ppm) due to its reduced viscosity, negligible nitrogen content, and enhanced burning velocity and turbulence intensity.

4. Conclusions

This study investigated the flame characteristics of biodiesel/Jet A-1 blends burned in a Lean Pre-vaporized Premixed (LPP) combustor, utilizing various burner designs with identical swirl numbers for flame stabilization. The biodiesel was produced from waste cooking oil using ultrasonic technology. The main conclusions are summarized below:

1. **Flame Stabilization:** Successful stabilization occurred in all experiments due to the interaction of shear layers, viscosity turbulence, and flame cavities formed in different flame zones.
2. **Flame Temperature:** The maximum flame temperature reached 1570 K at the B10 blend, where a spherically symmetric flame forms around the droplet. Fuel and oxidant vapors diffuse radially, leading to stoichiometric reactions at the flame front.
3. In this study, we experimentally investigated exit temperature, carbon monoxide (CO), oxygen (O₂) concentration, and nitrogen oxides (NO_x) emitted from a fixed swirl burner using Waste Cooking Oil Methyl Ester (WCOME) as fuel. Parameters examined included blend ratio (BR), fuel flow rate (\dot{m}_{fuel}), and local equivalence ratio (ϕ_{local}) approaching stoichiometry. Results indicated that increasing the blend ratio (BR), which corresponds to a higher WCOME ratio, led to a decrease in lower unit and a subsequent reduction in temperature. Additionally, carbon monoxide concentrations were linked to lower temperatures.
4. The B10D40 blend demonstrated a 38.80% reduction in CO emissions, a 58% reduction in NO_x emissions, and a 56.014% decrease in temperature, compared to pure Jet A-1 fuel at the combustion outlet. In contrast, the B5D40 blend showed a 44.54% reduction in CO emissions, a 38.06% reduction in NO_x emissions, and a 60% decrease in temperature compared to Jet A-1 fuel. Notably, Jet A-1 fuel achieved a higher maximum temperature than the other blends.

5. Additionally, the B5 and B10 blends exhibited relative variations in flame temperature distribution, whereas the diethyl ether blends displayed a temperature distribution similar to that of Jet A-1.
6. verall, the mixtures of B10D40 and B5D40 show significant potential for reducing emission levels. It can be concluded that a diethyl ether blending ratio of 40% is recommended for optimizing emission levels and flame temperature profiles.

References

- [1] Abas N, Kalair A and Khan N 2015 Review of fossil fuels and future energy technologies *Elsevier Futures* **69** 31-49
- [2] Afonja A A 2020 Fossil fuels and the environment *Books google.com*
- [3] Abbasi K R, Shahbaz M, Zhang J, Irfan M and Alvarado R 2022 Analyze the environmental sustainability factors of China: The role of fossil fuel energy and renewable energy *Renewable Energy* **187** 390-402
- [4] Mahmudul H M, Hagos FY, Mamat R, Adam A A, Ishak W F W and Alenezi R 2017 Production, characterization and performance of biodiesel as an alternative fuel in diesel engines—A review *Renewable Sustainable Energy Reviews* **72** 497-509
- [5] CaO C O I L U 2024 Fuel properties and emission characteristics of biodiesel fuel produced from waste *Journal of Ghana Science Association*
- [6] Singh D, Sharma D, Soni SL, Sharma S, Sharma P K and Jhalani A 2020 A review on feedstocks, production processes, and yield for different generations of biodiesel *Fue* **262** 116553
- [7] Mahlia T M I, Ismail N, Hossain N, Silitonga A S and Shamsuddin A H 2019. Palm oil and its wastes as bioenergy sources: a comprehensive review *Environmental Science and Pollution Research* **26** 14849-14866
- [8] Renzaho A M, Kamara J K and Toole M 2017 Biofuel production and its impact on food security in low and middle income countries: Implications for the post-2015 sustainable development goals *Renewable and Sustainable Energy Reviews* **78** 503-516
- [9] Neupane D, Bhattarai D, Ahmed Z., Das B, Pandey S, Solomon J K Q and Adhikari P 2021 Growing Jatropha (*Jatropha curcas* L.) as a potential second-generation biodiesel feedstock *Inventions* **6**(4), 60
- [10] Ruatpuia J VL, Halder G, Vanlalchhandama M, Lalsangpuii F, Boddula R, Al-Qahtani N and Rokhum S . 2024 Jatropha curcas oil a potential feedstock for biodiesel production: A critical review *Fuel* **370** 131829
- [11] Zhang H, Li Y and Zhu J K 2018 Developing naturally stress-resistant crops for a sustainable agriculture *Nature plants* **4**(12) 989-996
- [12] Abbasi M, Pishvae MS and Mohseni S 2021 Third-generation biofuel supply chain: A comprehensive review and future research directions *Journal of Cleaner Production* **323** 129100
- [13] Hasan MM and Rahman MM 2017 Performance and emission characteristics of biodiesel–diesel blend and environmental and economic impacts of biodiesel production: A review *Renewable and Sustainable Energy Reviews* **74** 938-948
- [14] Hassa C 2013 Partially premixed and premixed aero engine combustors *Gas Turbine Emissions* **38** 237
- [15] Enweremadu CC and Rutto HL 2010 Combustion, emission and engine performance characteristics of used cooking oil biodiesel—A review *Renewable and sustainable energy reviews* **14**(9) 2863-2873
- [16] Jiaqiang E, Pham M., Zhao D, Deng Y, Le DH., Zuo W and Zhang Z 2017 Effect of different technologies on combustion and emissions of the diesel engine fueled with biodiesel: A review *Renewable and Sustainable Energy Reviews* **80** 620-647
- [17] Liu Y, Sun X, Sethi V, Nalianda D., Li YG and Wang L 2017 Review of modern low emissions combustion technologies for aero gas turbine engines *Progress in Aerospace Sciences* **94** 12-45

- [18] Nemitallah MA, Rashwan SS, Mansir IB, Abdelhafez AA and Habib MA 2018 Review of novel combustion techniques for clean power production in gas turbines *Energy & Fuels* **32**(2) 979-1004
- [19] Siddique K 2018 Kinetics and decomposition mechanisms of selected Nitrogen-containing species *Doctoral dissertation, Murdoch University*
- [20] Pan W and Guo R 2024 The Harm of NO_x and its emission. In low-temperature selective catalytic reduction catalysts *Springer Nature Singapore* pp 1-9
- [21] Ahn SY, Go SM, Lee KY, Kim TH, Seo SI, Choi GM and Kim D J 2011 The characteristics of NO production mechanism on flue gas recirculation in oxy-firing condition *Applied Thermal Engineering* **31**(6-7) 1163-1171
- [22] Fernando S, Hall C and Jha S 2006 NO_x reduction from biodiesel fuels *Energy & Fuel* **20**(1) 376-382
- [23] Ding YQ., Chen ZY, Zhang FX and Ma JB. 2023 Coupling of N₂ and O₂ in the gas phase to synthesize nitric oxide at room temperature: A Zeldovich-Like Strategy *The Journal of Physical Chemistry Letters* **14**(34) 7597-7602
- [24] Garin F 2001 Mechanism of NO_x decomposition *Applied Catalysis A: General* **222**(1-2) 183-219
- [25] Xu S, Tian, Z and Liu H 2024 Development of a skeletal mechanism with NO_x chemistry for CH₄/H₂ combustion over a wide range of hydrogen-blending ratios *Energy & Fuels* **38**(20) 19758-19777
- [26] Gomez Escudero I 2023 Flame characterization and NO_x emissions prediction for reactors generated by Aeroengine-Derived lean direct injectors, operated on hydrogen and hydrogen/natural gas blends (*Doctoral dissertation, UC Irvine*)
- [27] Chawla M 2021 Carbon monoxide: Risk assessment, environmental, and health hazard. In Hazardous Gases *Academic Press* (pp 83-96)
- [28] Wild F 2003 Characterization of organic compounds *book Google com - CUP Archive*
- [29] Dey S and Dhal GC 2019 A review of synthesis, structure and applications in hopcalite catalysts for carbon monoxide oxidation *Aerosol Science and Engineering* **3**(4) 97-131
- [30] Krishnamoorthi M, Malayalamurthi R., He Z and Kandasamy S 2019 A review on low temperature combustion engines: Performance, combustion and emission characteristics *Renewable and Sustainable Energy Reviews* **116** 109404
- [31] Foo WH, Koay SSN, Chia, SR., Chia WY, Tang DYY, Nomanbhay S and Chew KW 2022 Recent advances in the conversion of waste cooking oil into value-added products: A review *Fuel* **324** 124539
- [32] Hua Y 2023 Ethers and esters as alternative fuels for internal combustion engine: A review *International Journal of Engine Research* **24**(1) 178-216
- [33] Venu H and Madhavan V 2017 Influence of diethyl ether (DEE) addition in ethanol-biodiesel-diesel (EBD) and methanol-biodiesel-diesel (MBD) blends in a diesel engine *Fuel* **189** 377-390
- [34] Osman S, Şara ON, Altun Kavaklı A and Lungu M J 2024 The effects of diethyl ether, diethylene glycol dimethyl ether, and dimethyl carbonate addition on the physical and thermodynamic properties of biodiesel *Journal of Thermal Analysis and Calorimetry* 1-25
- [35] Guan Y, Liu W and Han D 2021 Comparative study on spray auto-ignition of di-n-butyl ether and diesel blends at engine-like conditions *Journal of Energy Resources Technology* **143**(4) 042302.